Обзор ArXiv/astro-ph, 19-25 апреля 2023 года

От Сильченко О.К.

Revisiting the black hole mass of M87* using VLT/MUSE Adaptive Optics Integral Field Unit data I.

Ionized gas kinematics

J. Osorno[1] ⋆, N. Nagar[1]⋆⋆, T. Richtler[1], P. Humire[2], K. Gebhardt[3], and K. Gultekin[4]

[1] Departamento de Astronomía, Universidad de Concepción, Barrio Universitario S/N, Concepción, Chile
[2] Max-Planck-Institut für Radioastronomie, Auf dem Hügel 69, 53121 Bonn, Germany
[3] Department of Astronomy, University of Texas at Austin, Austin, TX 78712-1205, USA
[4] Department of Astronomy, University of Michigan, Ann Arbor, MI 48109, USA

ABSTRACT

Context. The stellar dynamic-based black hole mass measurement of M87 is twice that determined via ionized gas kinematics; these values disagree by more than 3σ. The former is closer to the mass estimated from the diameter of the gravitationally-lensed ring around the black hole.

Aims. Using a deeper and more comprehensive ionized gas kinematic dataset, we aim to better constrain the complex morphology and kinematics of the nuclear ionized gas, thus gaining insights into the reasons behind the disagreement of the mass measurements.

Methods. We use new Narrow Field Mode with adaptive optics, and Wide Field Mode integral field spectroscopic data from the *Multi Unit Spectroscopic Explorer* instrument on the *Very Large Telescope*, to model the morphology and kinematics of multiple ionized gas emission lines (primarily $H\alpha$+[N II] $\lambda\lambda6548,6583$ and [O I] $\lambda6300$) in the nucleus of M87.

Results. The new deep dataset reveals complexities in the nuclear ionized gas kinematics which was not seen in earlier sparse and shallower *Hubble Space Telescope* spectroscopy. Several ionized gas filaments, some with large flow velocities, can be traced down
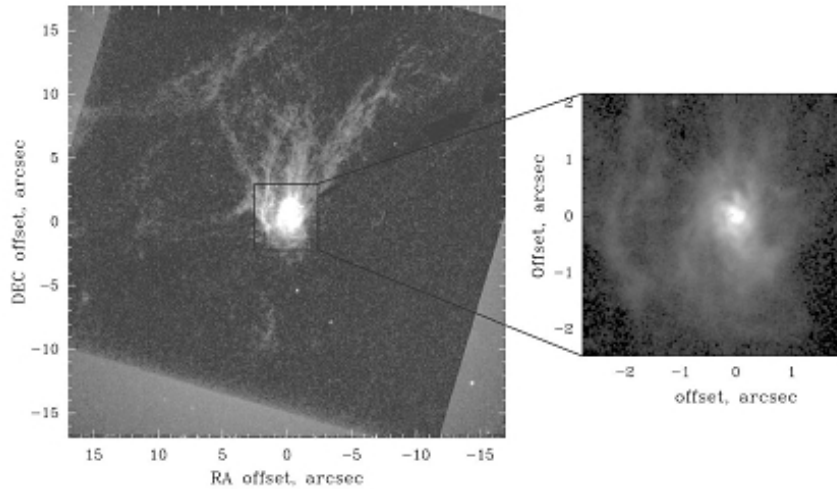
Газовый диск в M 87: HST

Figure 20. A WFPC Hα map of M87. The inset to the left shows details of the nuclear dust disk. From Ford et al. (1994).
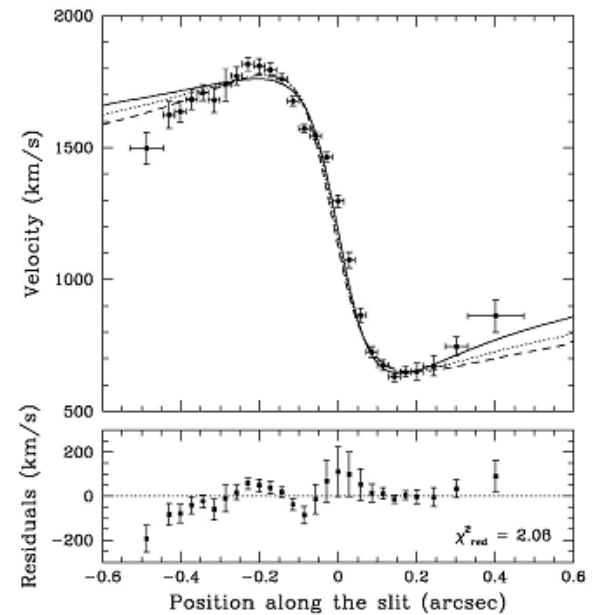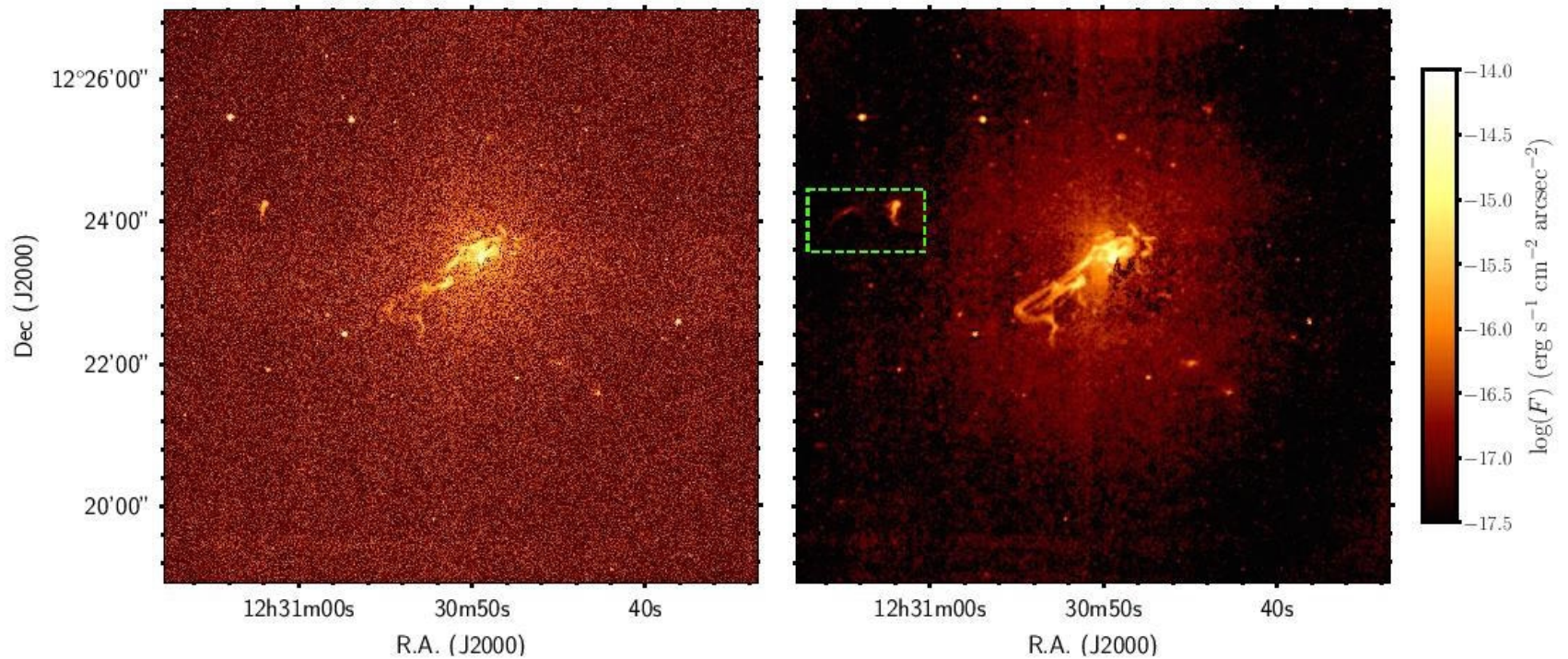

Figure 21. The *HST*/FOC rotation curve of the ionized gas disk in M87 (from Macchetto et al. 1997). The different lines correspond to different model fits to the data; all require the presence of a central black hole of a few 10^9 M$_\odot$, but differ slightly in the other parameters, most notably the position angle of the disk's line of nodes.
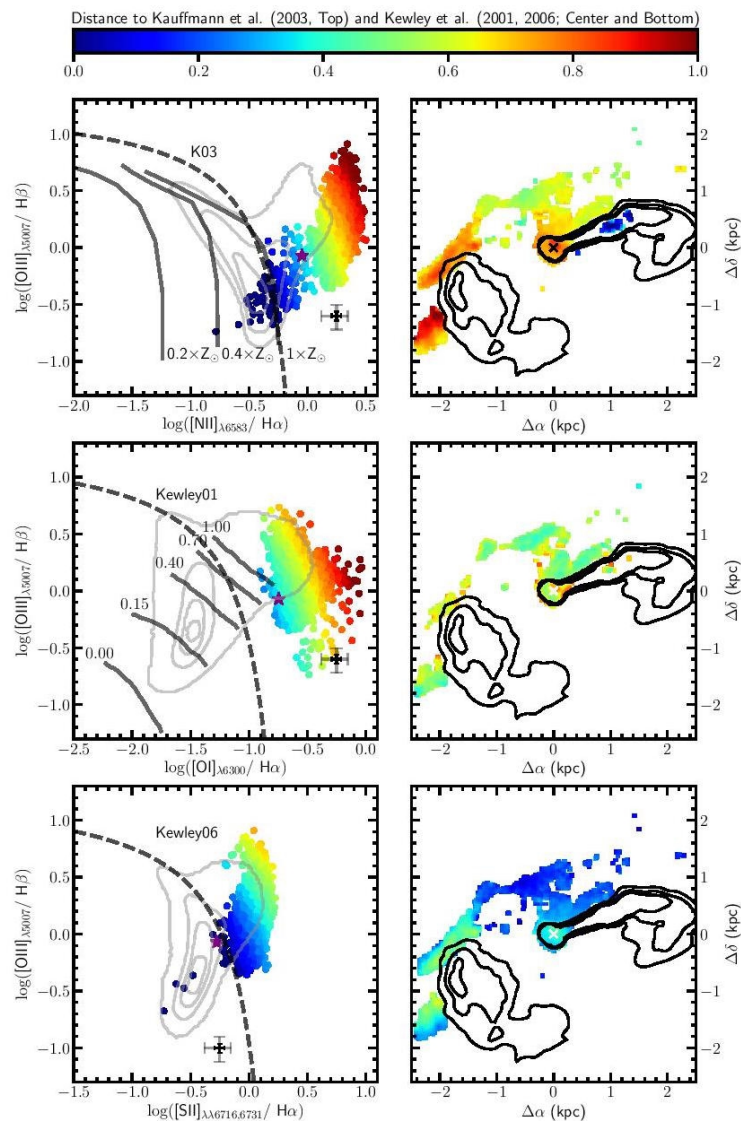
VLT/MUSE

Boselli+ 2019

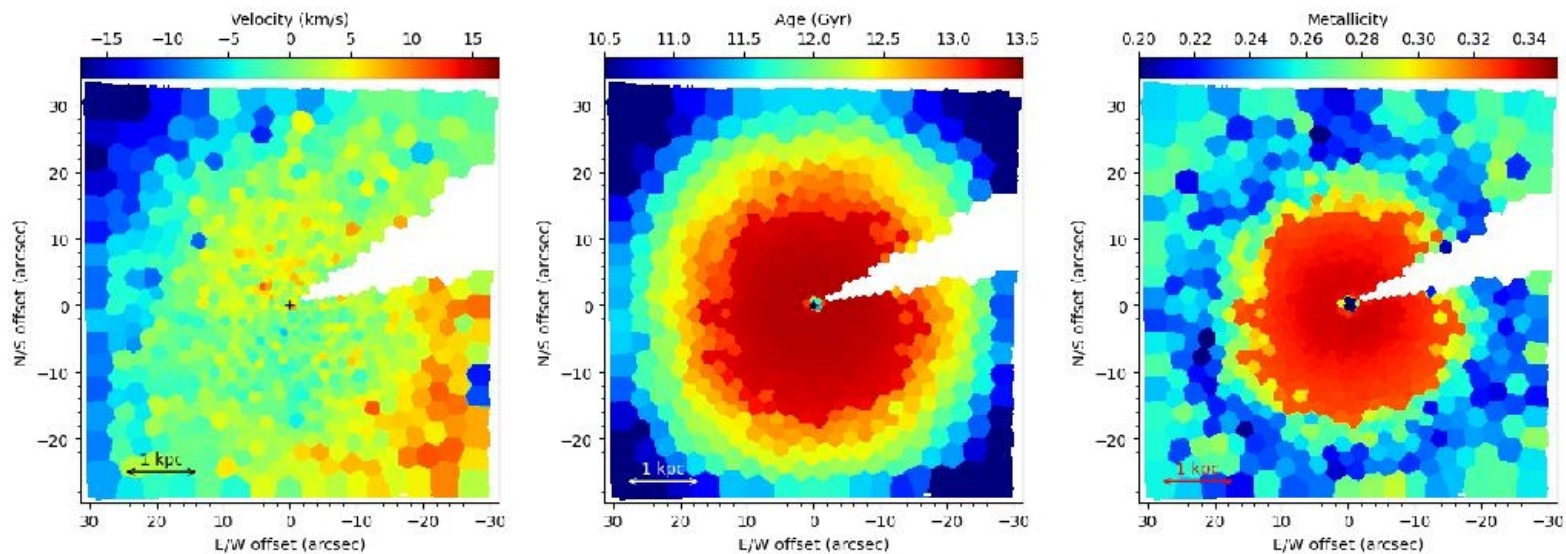# Поле скоростей ионизованного газа+изофоты джета
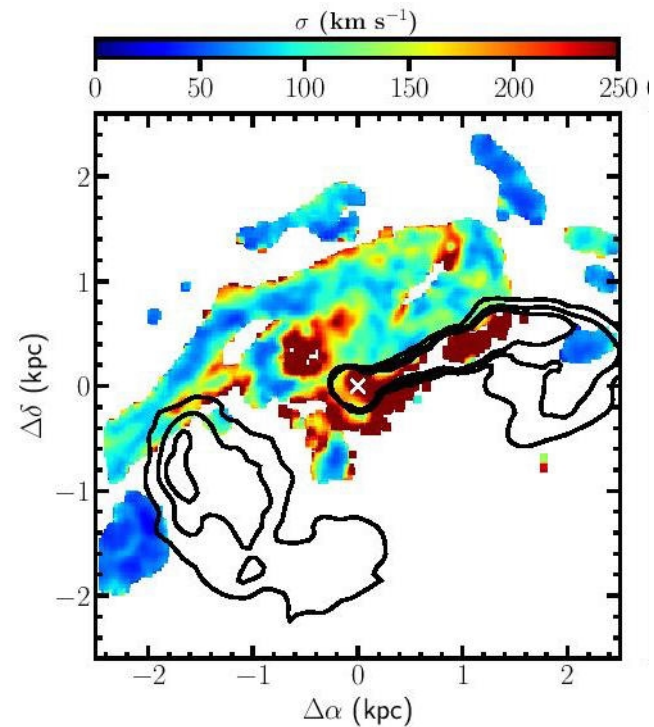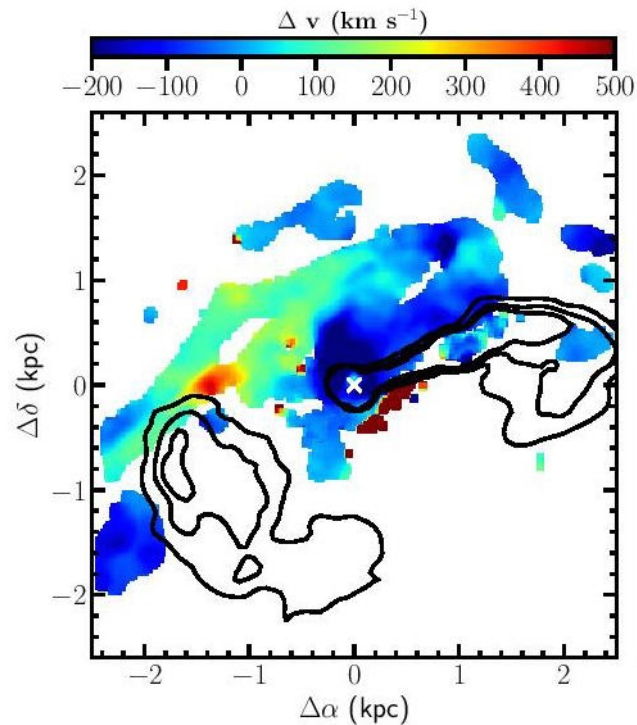
Boselli+2019

# Но тогда их больше интересовало возбуждение…

Boselli+2019

А теперь полная переработка куба данных MUSE: звезды

Fig. 1. Maps of stellar properties derived with the *GIST Pipeline* run on the MUSE WFM datacube. Left: stellar velocity map; zero velocity corresponds to a radial velocity of 1313 km s^{-1}. Middle: map of the weighted mean stellar age of the best-fit templates. Right: map of the weighted mean metallicity of the best-fit templates. These maps were derived using *GIST Pipeline* over a wavelength range of 5050 – 6000 Å, with Voronoi binning used to obtain a SNR $\geq$ 300 in each bin. All spaxels with significant jet emission were masked in the datacube to avoid confusion.

А теперь полная переобработка куба данных MUSE: газ
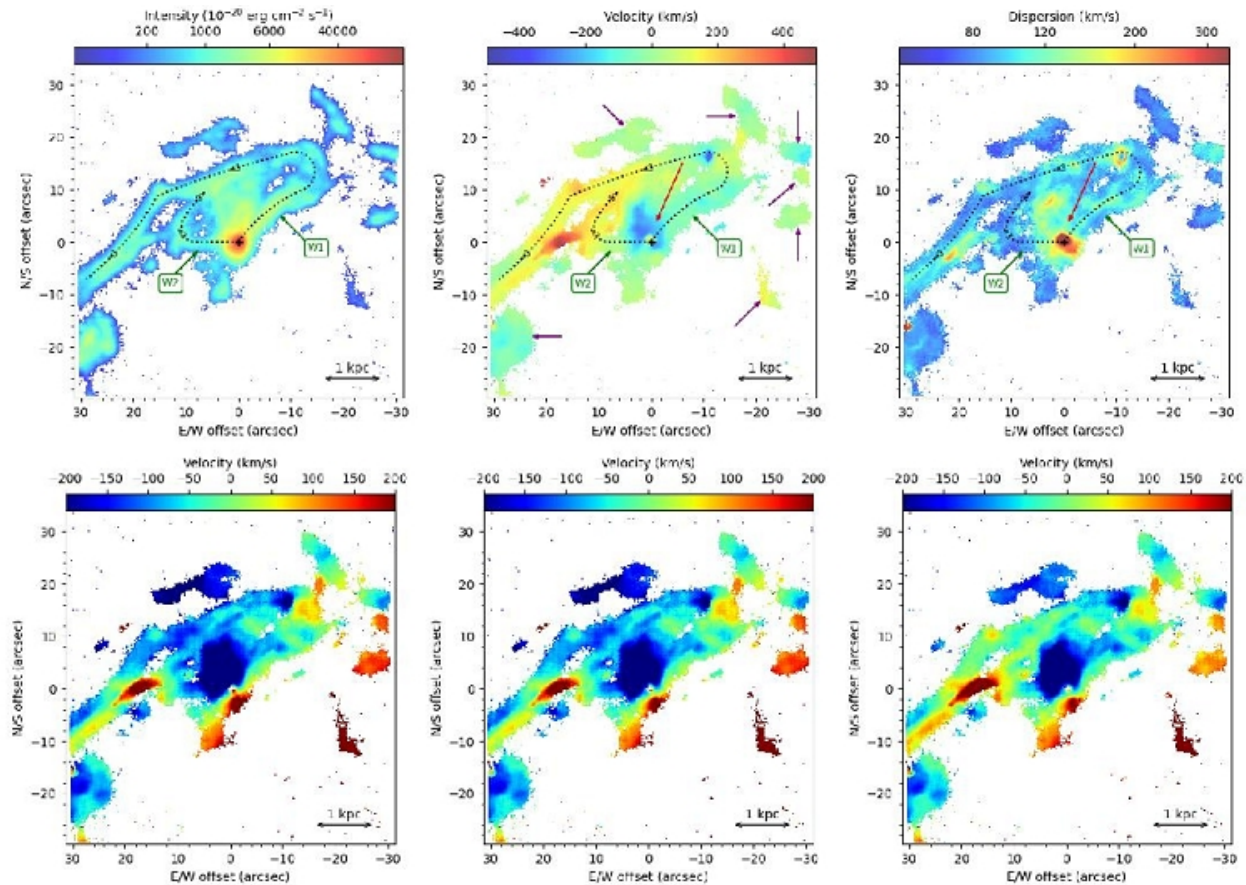
Fig. 2. Top: moment maps for the [N II] λ6583 line as derived from Gaussian fits to the MUSE WFM datacube. Left to right are the total intensity, velocity, and dispersion maps. Two ionized gas filaments (black dotted lines) are indicated by green arrows and the labels W1 and W2; these dotted lines are the pseudo-slits along which the pv diagrams of Fig. 3 are extracted. Several ionized gas bubbles are indicated by purple arrows and the position of the outflow is indicated by a red arrow. Bottom: residual velocity maps of the [N II] λ6583 line in the MUSE WFM datacube. These maps, discussed in Sect. 5.2.1, show the residual velocity field after subtracting a model of a rotating thin nuclear disk (in a SMBH plus stellar potential) for a black hole and nuclear disk with the following parameters (M•, disk position angle, disk inclination): left: 6.6×10^9 M⊙ (G11), 45° and 42°; middle: 3.5×10^9 M⊙ (W13), 45° and 42°; and right: 6.6×10^9 M⊙ (G11), 40° and 25° (see Sect. 5.2.1).

PV-диаграммы вдоль двух «кривых» разрезов - филаментов
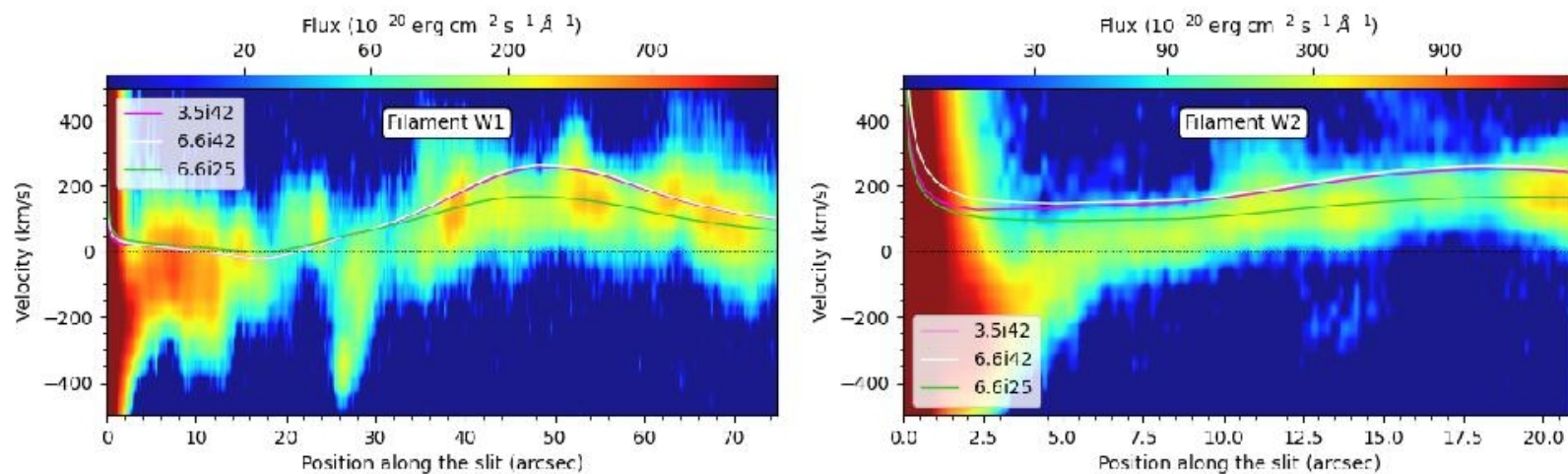
Fig. 3. Position-velocity diagrams of the [N II] λ6583 line for pseudo-slits along the gas filaments W1 and W2 identified in Fig. 2. The x axis zero position of each filament corresponds to the black cross in Fig. 2. The three curves are the expected disk rotation velocities with the parameters described in Sect. 5.2.1 and Fig. 2, with colors as listed in the insert. At offsets beyond 10″, the velocities of both filaments are best fit with the i=25° model. This figure is discussed in Sect. 5.2.1, but placed here for easy comparison with Fig. 2.

Новые наблюдения – с адаптивной оптикой (разрешение 0.1'')
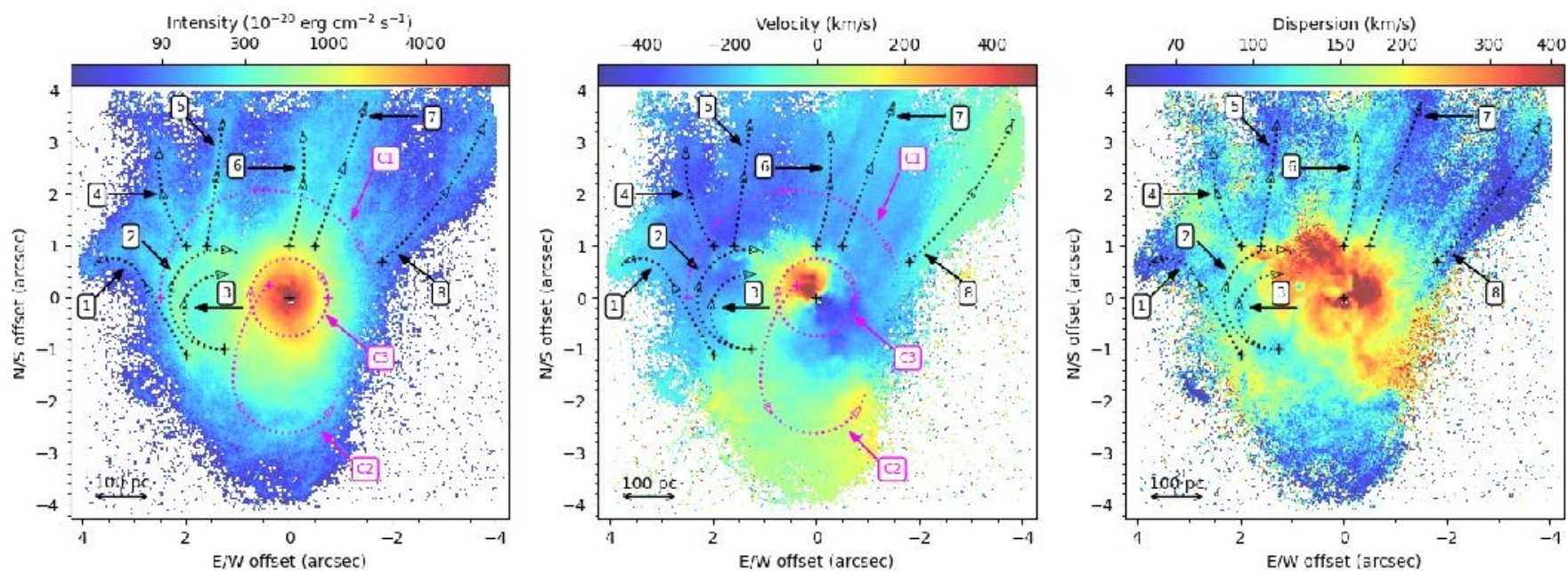
Fig. 4. [N II] $\lambda6583$ emission line moment maps from Gaussian fits to the NFM cube: left to right are maps of the total intensity, velocity, and velocity dispersion. Eight ionized gas filaments (black dotted lines), and three pseudo-slits (magenta dotted lines), are numbered and indicated with arrows of the same color in all panels.

Еще PV-диаграммы
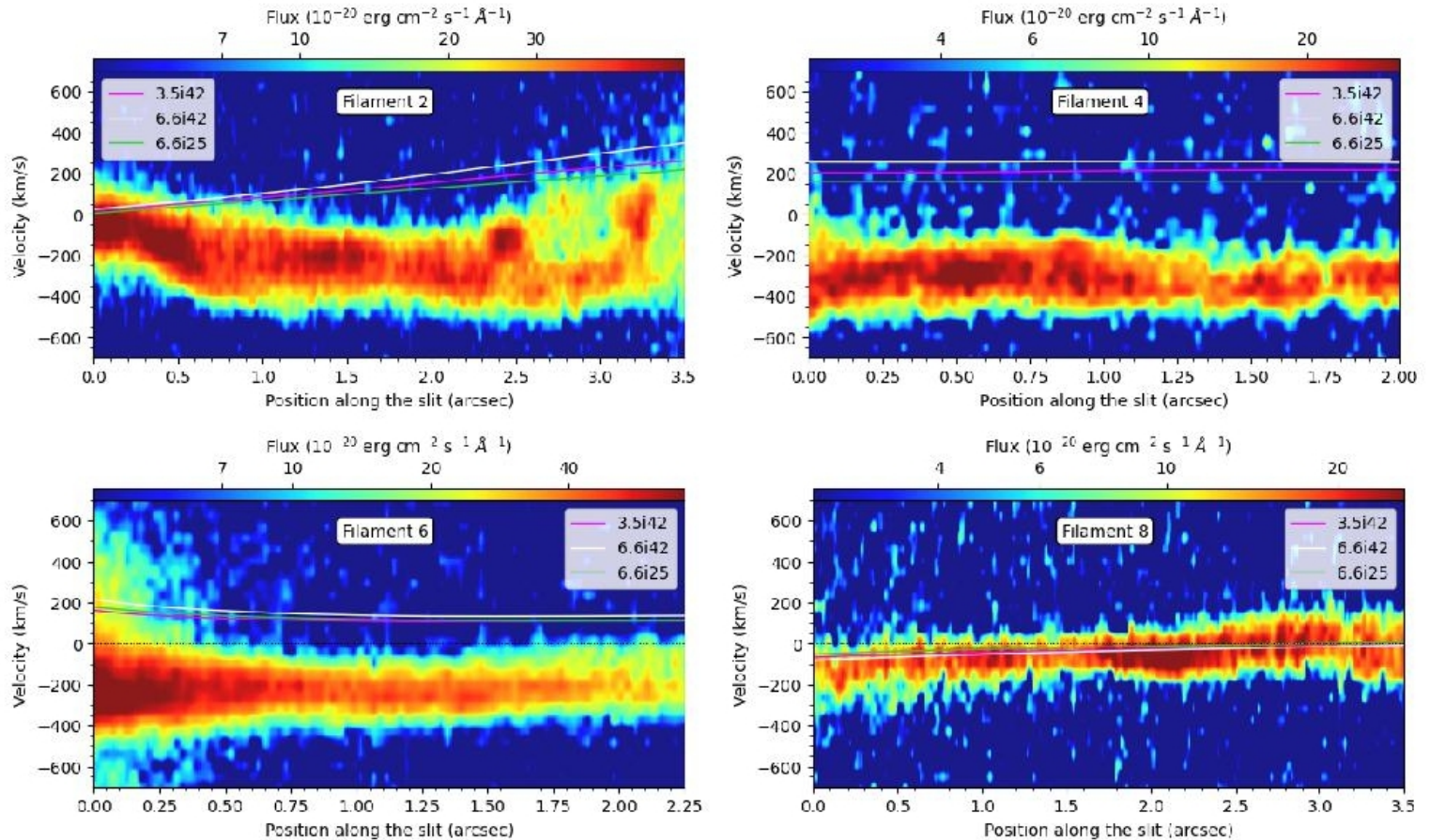
Fig. 5. As in Fig. 3 but for four of the eight filaments marked with black dotted curves in the NFM moment maps of Fig. 4. The remaining four filaments are presented in Fig. C.1. These pv diagrams are discussed in Sect. 5.2.2, but are placed here for easy comparison with Fig. 4.
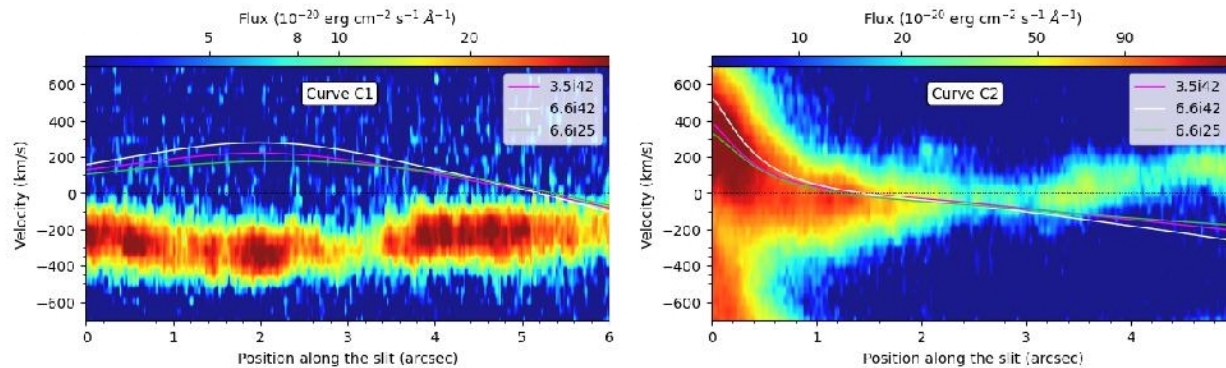
Еще PV-диаграммы

Fig. 6. As in Fig. 3 but for pseudo-slits C1 and C2 marked in magenta dotted curves in the moment maps of Fig. 4.
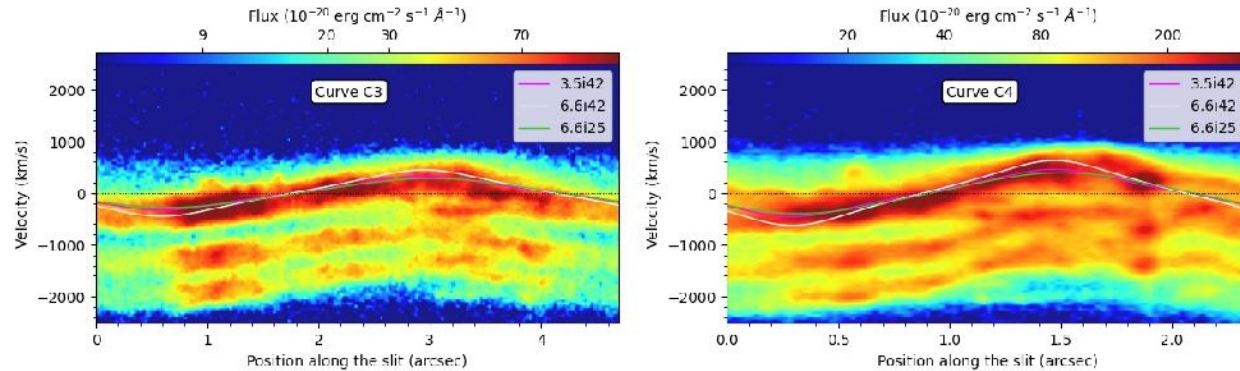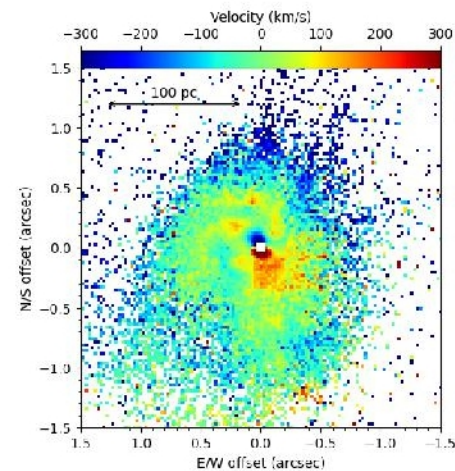

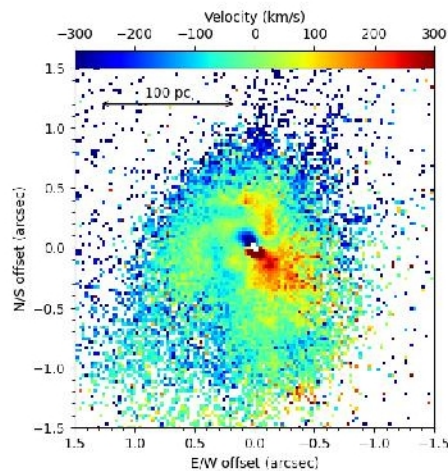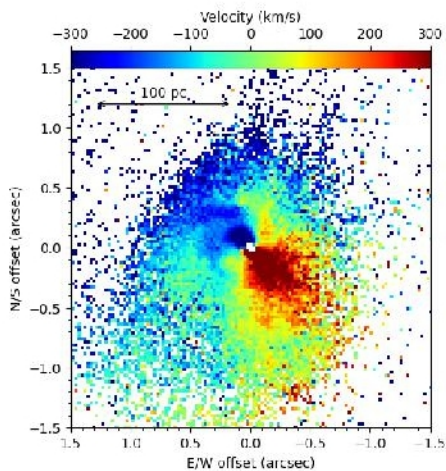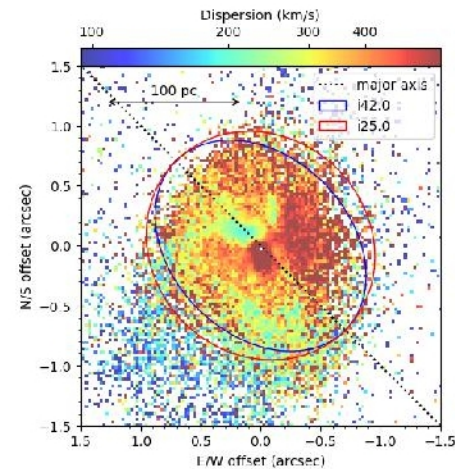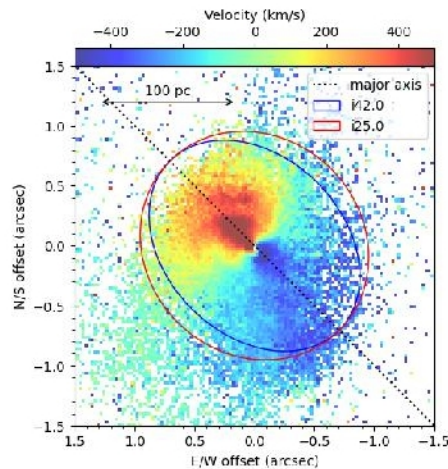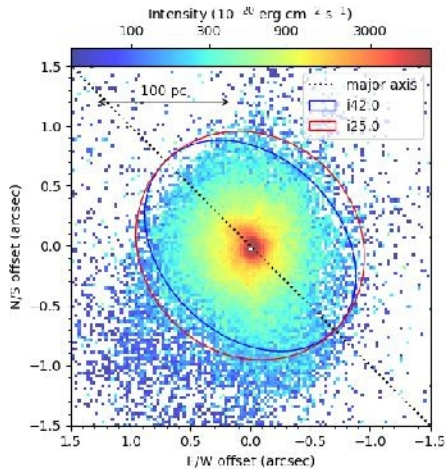**Fig. 7.** Left: as in Fig. 3 but for the pseudo-slit C3 (nuclear radius 0."75") marked with a magenta dotted line in the left and central panels of F... 4. Right: as in the left panel, but for a circular pseudo-slit at a nuclear radius of 0."375; a larger range of velocities is shown in order to show t... full Hα+[N II] line complex.
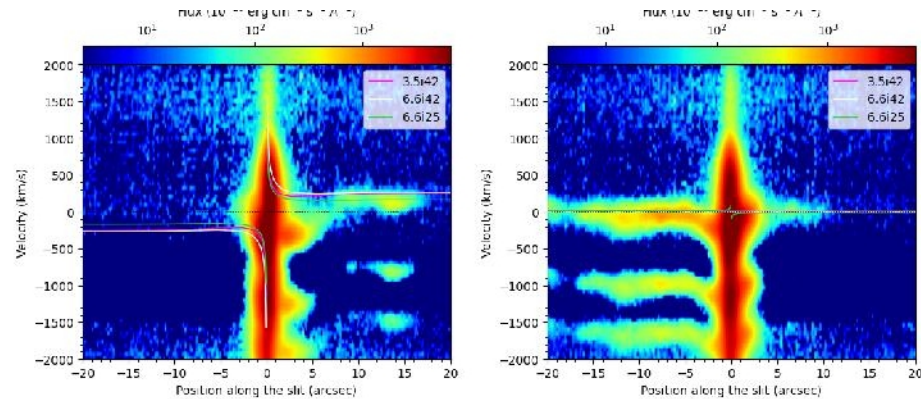
Для самого центра – [OI]6300

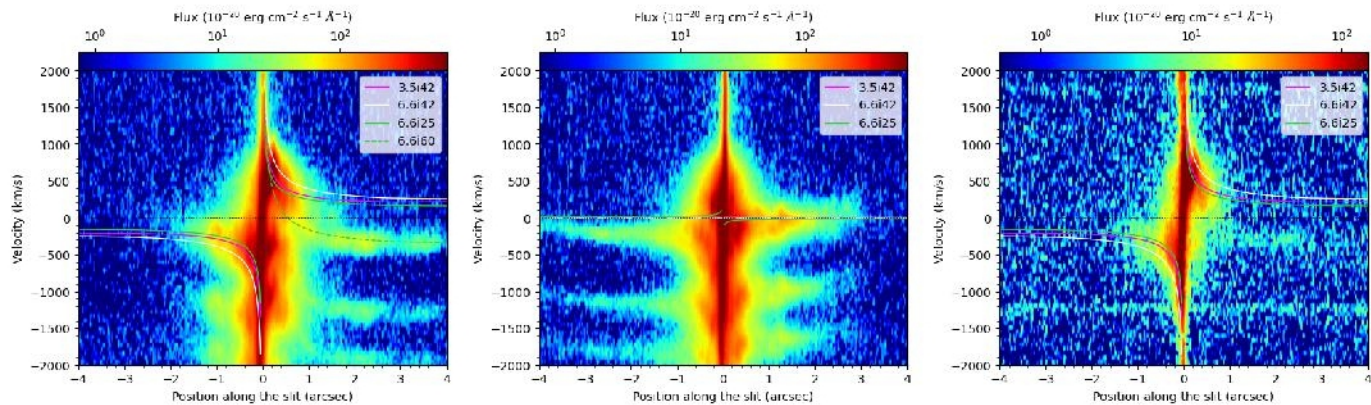# Еще PV – вдоль большой и малой осей

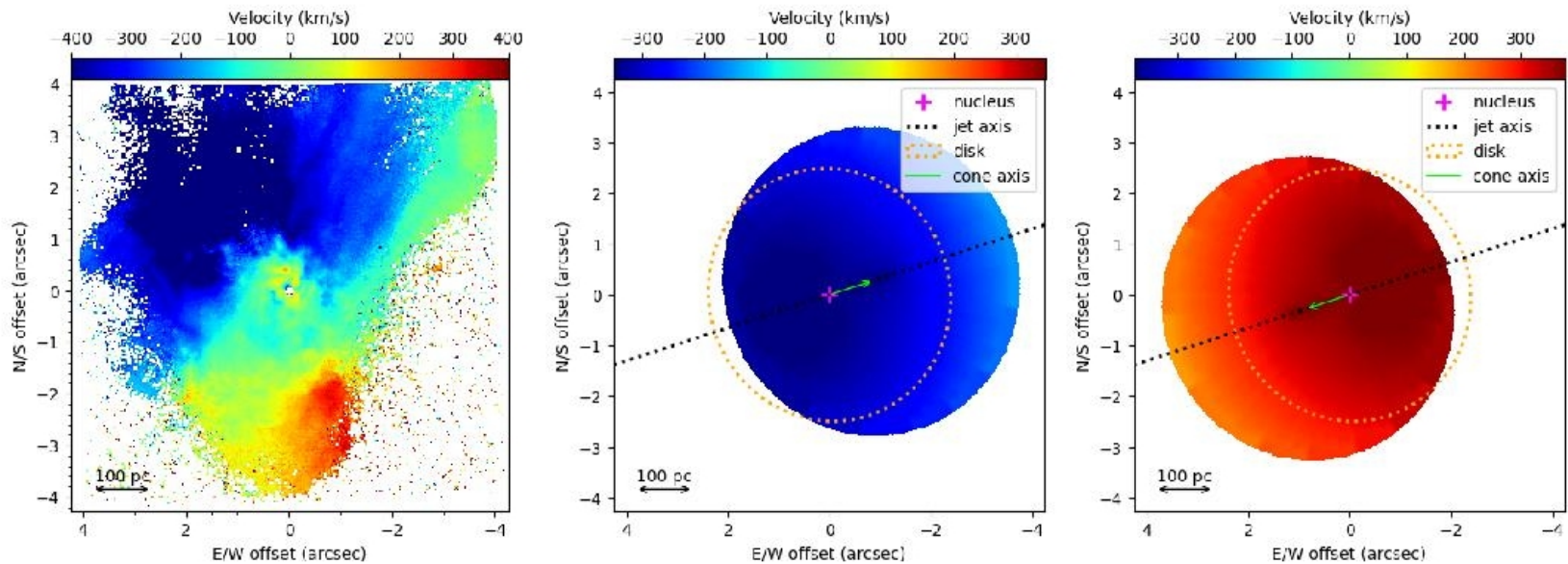**Fig. 10.** PV diagrams of the Hα+[N II] λλ6548,6583 lines in the WFM cube along the W13 major (45°, left) and minor axes (135°, right). The models (see inset) and the 'zero' velocity are plotted with respect to the [N II] λ6583 line.

Fig. 11. PV diagrams of the Hα+[N II] λλ6548,6583 (left and central) and [O I] (right) emission lines in the NFM cube, along the W13 major

Истечение газа

Fig. 13. Left panel: The residual (after subtracting the 6.6i25 model for the nuclear disk) [N II] velocity map. Note the gradients in the blue and redshifted velocities to the NE and S. Middle and right panels: models of a filled conical outflow made with *KinMSpy*, with each cone showed separately. The cone half-opening angles are 45° (approaching; middle panel) and 30° (receding; right panel). Each cone has an extent of 3″ along its axis, and the radial outflow velocity within each cone is 400 km s^{-1}. The inclination of both cone axes to the line of sight is 18°. The green line shows the projection of the cone axes on the plane of the sky; these project to PA 288°, the PA of the jet axis. The orange dotted lines delineate the projected shape of a disk perpendicular the cone axes.